16th World Conference on Earthquake Engineering, 16WCEE 2017
Santiago Chile, January 9th to 13th 2017
Paper N° 4389 (Abstract ID)
Registration Code: S-O1464683704

IDENTIFICATION AND FINITE ELEMENT MODELING OF ALCAZAR BUILING IN CHILE USING EARTHQUAKE VIBRATION DATA

C. Papadimitriou[1], I. Gavriilidis[2], C. Argyris[3], H. Jensen[4], C. Esse[5], V. Araya[6]

[1] Professor, Department of Mechanical Engineering, University of Thessaly, Greece, costasp@uth.gr
[2] Undergraduate Student, Department of Mechanical Engineering, University of Thessaly, Greece, ilgavrii@uth.gr
[3] Ph.D. Student, Department of Mechanical Engineering, University of Thessaly, Greece, koargiri@uth.gr
[4] Professor, Department of Civil Engineering, Santa Maria University, Valparaiso, Chile, hector.jensen@usm.cl
[5] MSc. Student, Department of Civil Engineering, Santa Maria University, Valparaiso, Chile, carlos.esse@alumnos.usm.cl
[6] MSc. Student, Department of Civil Engineering, Santa Maria University, Valparaiso, Chile, victor.arayan@alumnos.usm.cl

Abstract

Earthquake vibration data collected from an instrumented structure contain important information for estimating the dynamic characteristics and updating models of the structure. In this work we use earthquake acceleration time histories from three low amplitude earthquake events recorded for the 16-story Alcazar building office in Viña del Mar (Chile) at the far field, basement and various floors, in order to identify the building's modal characteristics (modal frequencies, modal damping ratios and mode shapes). For this, modal identification techniques developed to handle non-classically-damped modes are outlined. A three-step modal identification approach is proposed. In the first step, conventional least squares complex frequency algorithms along with stabilization diagrams are used to automatically estimate the modal frequencies and the damping ratios of the modal model and to distinguish between the physical and mathematical modes. In the second step, two approaches are proposed for computing the mode shapes and the effective participation factors, one very efficient one which does not require iterations, and an iterative one that uses the estimates of the first approach as initial values to accelerate convergence. In order to improve the estimates for closely-spaced and overlapping modes, the full nonlinear optimization problem is solved in the third step by using the initial estimates of the parameters obtained in the first two steps. The modal properties are useful in updating finite element (FE) models. A high-fidelity FE model is also developed in SAP and the modal properties are compared with the ones identified using the measurements. Up to 7 modes were reliably identified from the analyses of the three seismic events. The lowest two bending modes in the EW direction, the three bending modes in the NS direction and the second torsional mode. Due to the sparse sensor grid, the type of some of the identified modes could not be easily estimated without the use of the FE model as a guide. For the majority of the identified modes, the damping ratios ranged from 2% to 3%. The modes were found to be very close to classically-damped modes. The analysis of the three events gave consistent results for the modal properties. Most of the modal frequencies have relatively small variation over the three seismic events. The values of the identified modal frequencies are close to the values predicted by the high-fidelity FE model. The modal frequency values predicted from the FE model are higher, indicating that the model is stiffer than the actual behavior of the building. The identified modes are representative of the condition of the building at low-amplitude vibration levels and can be further used for model updating, linear and nonlinear analyses, as well as structural health monitoring purposes. Matching the mode shapes in an FE model updating methodology presents challenges mostly from the fact that there is no measurements available from the 7th up to the 16th floor of the structure. FE model updating using hierarchical Bayesian modeling to account variabilities from the different seismic events is left for a future work.

Keywords: Modal identification; buildings; seismic excitation; vibration measurements;

1. Introduction

The evaluation of the actual dynamic characteristics of engineering structures through measurements of their dynamic response has been attracting an increasing research effort worldwide. Measured response data of civil engineering structures (e.g. bridges, buildings, dams, towers) from earthquake-induced vibrations, and vehicles from vibrations induced by road roughness, offer an opportunity to study quantitatively and qualitatively their dynamic behavior within the resulting vibration levels. These vibration measurements can be processed for the estimation of the modal characteristics of these structures, as well for the calibration of corresponding FE models used to simulate their behavior. The information for the identified modal models and the updated FE models is useful for validating the assumptions used in model development or for improving modelling, analysis and design procedures. Also, such information is useful for structural health monitoring purposes.

This work is concerned with the development methods for identifying the modal characteristics of civil infrastructure based on vibration measurements that are caused by earthquakes. The evaluation of the actual dynamic characteristics of engineering structures through measurements of their dynamic response has been attracting an increasing research effort worldwide [1-9]. For earthquake-induced vibrations on civil structures, the modal characteristics are estimated from the measured acceleration excitations occurred at the multiple supports of the structure and the measured vibration responses. It has been observed from response measurements of these structures that their dynamic properties are markedly different during response to strong motion than in small amplitude ambient and forced vibration tests. Hence, it is of considerable interest and importance to extract information about structural behavior from small amplitude and strong motion data.

Modal identification algorithms provide estimates of the modal frequencies, modal damping ratios, modal participation factors and mode shapes at the measured DOFs using classically-damped or non-classically damped modal models. For the case of earthquake-induced vibrations, modal identification methods have been developed in time [10] and frequency domains [11], based on a minimization of the measure of fit between the time history or its Fourier transform of the acceleration responses estimated from the measurements and the corresponding ones predicted from a classically-damped modal model of the structure. Beck and Jennings [10] has presented an output-error approach for the identification of linear, time-invariant models from strong motion records, through the minimization of a measure of fit including displacement, velocity and acceleration records. McVerry [11] has applied an output-error approach in the frequency domain, using the Fast Fourier Transform of the acceleration response time histories to estimate the modal properties through least-squares matching. These methods have been applied to identify the modal characteristics of bridges [1,7] and buildings [12] by processing input-output earthquake recordings. Werner et al. [1] formulated a methodology in the time domain for the case of measured input excitation, such as earthquake excitation, for an elastic system with classical normal modes and with motion measurements from any number of input and system response degrees of freedom (DOF). Their procedure was an extension of the least-squares-output-error method which was used in [10].

Extensions for identifying non classically-damped modal models in the frequency domain have also been developed by Chaudhary et al. [6]. Tan and Cheng [13] proposed an iterative identification algorithm, which was based on the modal sweep concept and the band-pass filtering process, to identify the modal parameters of a non-classically damped linear structure from its recorded earthquake response. Mahmoudabadi et al. [14] developed a method for parametric system identification in frequency domain for classically and non-classically damped linear systems subjected up to six components of earthquake ground motions, which is able to work in multi-input/multi-output (MIMO) case.

The methods developed in [11] in the frequency domain and in [10] in the time domain, are extended in this work to treat non-classically damped modal models, since damping may not be proportionally distributed in various structural components. For the special case of bridges, non - proportionally damping appears due to the energy dissipation mechanism provided locally by the elastomeric bearings and the foundation soil. For base isolated buildings, non-proportional damping may appear due to the energy dissipation mechanism provided locally by the isolation system. Least-squares output-error methods are used in which the optimal values of the modal parameters are obtained by minimizing the discrepancy between measured responses and the predicted

responses of the system. Time domain output error methods process the response time histories measured from a network of sensors (e.g. accelerometers), while frequency domain output error methods process the Fourier transforms of the measured response time histories.

A novel aspect of this study is the use of a three step approach to solve the resulting highly non-convex nonlinear optimization problem. The first step provides estimates of the modal frequencies and modal damping ratios by solving a system of linear algebraic equations. Stabilization diagrams are used to identify the number of contributing modes by distinguishing between physical and mathematical modes. The second step provides estimates of the mode shapes and the participation factors by solving a system of linear algebraic equations for the modal residue matrices of the contributing modes and using singular value decomposition to estimate the complex mode shapes and modal participation factors. The first two steps usually give accurate estimates of the modal characteristics. A third step is added to improve the estimates of the modal characteristics by efficiently solving the full nonlinear optimization problem with initial estimates of the modal parameters those obtained from the first and second steps. The gradients of the objective function with respect to the parameters are obtained analytically in order to significantly accelerate the convergence of the optimization in the third step. The effectiveness of the proposed methodology has been confirmed using simulated data from simplified structural models, as well as earthquake recordings available from a full-scale reinforced concrete bridges, reinforced concrete structures and a cable-stayed bridge [15]. Herein it is applied a sixteen-story reinforced concrete building office located in the city of Viña del Mar, Chile, in order to identify its modal characteristics and their variabilities using available earthquake recordings from three seismic events. The identified results are also compared with the modal characteristics obtained from a 60000-DOF high fidelity model of the building and useful conclusions are drawn.

2. State Space Formulation of Equations of Motion

Consider a structure that is subjected to multiple base excitations. The equations of motion, assuming that the structure behave linearly, can be derived using a FE analysis. Let $M \in R^{n\times n}$, $C_0 \in R^{n\times n}$ and $K \in R^{n\times n}$ be the fixed-support mass, damping and stiffness matrices, respectively, $\underline{y}_s(t) \in R^n$ be the response at the DOFs of the mathematical model of the structure and $\ddot{\underline{z}}(t) \in R^{N_{in}}$ be the displacement of the supports DOFs, where n is the number of model DOFs and N_{in} is the number of excitation DOFs at the supports (bases). The response $\underline{y}_s(t)$ of the structure is given by [1,16]

$$\underline{y}_s(t) = \underline{s}(t) + \underline{q}(t) \tag{1}$$

where $\underline{s}(t)$ is the pseudo static component and $\underline{q}(t)$ is the dynamic component of the response. The pseudo static component of the response represents the 'static' contributions of the individual support motions to the system response and it is given by $\underline{s}(t) = D\,\underline{z}(t)$, where $D = -K^{-1}K_{sb}$ is the pseudo static matrix, which expresses the responses in all DOF due to unit support motions, where K_{sb} is the stiffness matrix that couples the system and base DOFs.

The dynamic component $\underline{q}(t)$ in (1) accounts for the contributions of the system's fixed-base modal vibrations about its pseudo static reference position. The equation of motion for the dynamic response is given by

$$M\,\ddot{\underline{q}}(t) + C_0\,\dot{\underline{q}}(t) + K\,\underline{q}(t) = L\,\ddot{\underline{z}}(t) \tag{2}$$

where $L = -(M\,D + M_{sg})$, and M_{sg} is the mass matrix that couple the system and base DOFs.

In the general case of a non-classically damped structure, the set of equations (2) must be converted to a set of first-order state space formulation. This is accomplished by introducing the state vector $\underline{x} = [\underline{q}^T \quad \underline{\dot{q}}^T]^T$. Equations (2) along with the complementary equation $M\,\underline{\dot{q}}(t) = M\,\underline{\dot{q}}(t)$ can be written in the state space form

$$P\underline{\dot{x}} + Q\underline{x} = \begin{bmatrix} L^T & 0^T \end{bmatrix}^T \underline{\ddot{z}}(t) \tag{3}$$

where the matrices P and Q are given by

$$P = \begin{bmatrix} C_0 & M \\ M & 0 \end{bmatrix}, \quad \mathrm{Q} = \begin{bmatrix} K & 0 \\ 0 & -M \end{bmatrix} \tag{4}$$

Let $\underline{y}(t) \in R^{N_{out}}$ be the observation vector containing the measured output acceleration responses

$$\underline{y}(t) = C_\alpha \underline{\ddot{y}}_s(t) = C_c \underline{x} + D_c \underline{\ddot{z}}(t) \tag{5}$$

where $C_\alpha \in R^{N_{out} \times n}$ is a matrix indicating which DOFs are measured (considered in the output measurements). Using (1) and (2) and the fact that $L = -(M\,D + M_{sg})$, the matrices C_c and D_c are given by $C_c = -C_\alpha M^{-1}[K \quad C_0] \in R^{N_{out} \times 2n}$ and $D_c = C_\alpha (M^{-1}L + D) = -C_\alpha M^{-1} M_{sb} \in R^{N_{out} \times N_{in}}$.

3. Non-Classically Damped Modal Models

Modal analysis is used to describe the response at the measured DOFs of the structure in terms of the complex eigenvalues and eigenvectors and the excitation. Let $\underline{\psi}_r \in \mathrm{C}^{2n}$ be the complex eigenvector and λ_r the corresponding complex eigenvalue satisfying the eigenproblem associated with the system (3), i.e.

$$(P\lambda + Q)\underline{\psi} = \underline{0} \tag{6}$$

Introducing the eigenmatrix $\Psi = \begin{bmatrix} \underline{\psi}_1 & \cdots & \underline{\psi}_n & \underline{\psi}_1^* & \cdots & \underline{\psi}_n^* \end{bmatrix} \in \mathrm{C}^{2n \times 2n}$, where the superscript <*> denotes complex conjugate, it can easily be shown that the eigenmatrix Ψ is partitioned in the form

$$\Psi = \begin{bmatrix} \Phi & \Phi^* \\ \Phi\Lambda & \Phi^*\Lambda^* \end{bmatrix} \in \mathrm{C}^{2n \times 2n} \tag{7}$$

where $\Phi \in \mathrm{C}^{n \times n}$ is the eigenmatrix associated with the displacement DOFs $\underline{q}(t)$ of the state vector $\underline{x}(t)$. The complex eigenvectors satisfy the orthogonality condition $\Psi^T P \Psi = diag[\alpha_r]$ and $\Psi^T P \Psi = diag[\beta_r]$. The matrix $\Lambda = diag(\lambda_r) \in \mathrm{C}^{n \times n}$ is a diagonal matrix with diagonal elements the complex eigenvalues $\lambda_r = -\beta_r / \alpha_r$ represented in the form

$$\lambda_r = -\zeta_r \omega_r \pm j\omega_r \sqrt{1-\zeta_r^2} = -a_r \pm jb_r, \qquad r = 1, \ldots, m \tag{8}$$

with the modal frequency ω_r and the modal damping ratio ζ_r satisfying $\omega_r = |\lambda_r|$ and $\zeta_r = -\mathrm{Re}\{\lambda_r\} / \omega_r$. The parameters $\alpha_r = \zeta_r \omega_r$ and $b_r = \omega_r \sqrt{1-\zeta_r^2}$ are expressed in terms of the modal frequency ω_r and the modal damping ratio ζ_r. Given α_r and b_r in (8), the modal frequency ω_r and the damping ratio ζ_r are obtained from the following relationships $\omega_r = \sqrt{a_r^2 + b_r^2}$ and $\zeta_r = a_r / \sqrt{a_r^2 + b_r^2}$.

For the realization of modal analysis method the following transformation is introduced

$$\underline{x}(t) = \Psi \begin{Bmatrix} \underline{\xi}(t) \\ \underline{\xi}^*(t) \end{Bmatrix} \tag{9}$$

where $\underline{\xi} = [\xi_1(t), \cdots, \xi_m(t)]^T \in \mathrm{C}^m$ is the vector of the main modal coordinates. Using conventional modal analysis, the vector $\underline{y}(t;\underline{\theta})$ in (5) of the acceleration responses at the N_{out} measured DOFs, based on the non-classically damped modal models, can be written in the form

$$\underline{\ddot{y}}(t) = U\underline{\xi}(t) + U^*\underline{\xi}^*(t) + D_c\underline{\ddot{z}}(t) = \sum_{r=1}^{m}[\underline{u}_r\xi_r(t) + \underline{u}_r^*\xi_r^*(t)] + D_c\underline{\ddot{z}}(t) \tag{10}$$

where the complex-valued modal coordinates $\xi_r(t)$, $r = 1, \cdots, m$, satisfy the complex modal state space equations

$$\dot{\xi}_r(t) = \lambda_r\xi_r(t) + \underline{l}_r^T\underline{\ddot{z}}(t) \tag{11}$$

$D_c = -C_\alpha M^{-1}M_{sb} \in R^{N_{out}\times N_{in}}$ is a real matrix,

$$U \equiv [\underline{u}_1, \cdots, \underline{u}_m] = C_c\begin{bmatrix} \Phi \\ \Phi\Lambda \end{bmatrix} = C_\alpha\Phi\Lambda^2 \in \mathrm{C}^{N_{out}\times m} \tag{12}$$

is the matrix of the complex eigenvectors $\underline{u}_r = \lambda_r^2 C_\alpha\underline{\phi}_r \in \mathrm{C}^{N_{out}}$, $r = 1, \cdots, m$, at N_{out} DOFs, and $\underline{l}_r^T = (1/\alpha_r)\underline{\phi}_r^T L \in \mathrm{C}^{1\times N_{in}}$ is the complex vector of the modal participation factors relating the N_{in} inputs to the r mode of the system. The modal response $\xi_r(t)$ can be obtained by solving (11) using the complex-valued initial condition $\xi_r(0)$.

Applying FT to both sides of (10) and (11), one can derive a relation between the Fourier Transform (FT) $\underline{\hat{y}}(\omega)$ of the response $\underline{y}(t)$ and the FT $\underline{\hat{\ddot{z}}}(\omega)$ of the excitation. Letting $\underline{y}_k(\underline{\theta})$ represents the Fourier transform $\underline{\hat{y}}(k\Delta\omega)$ of the acceleration response $\underline{y}(t)$ at frequency component $\omega = k\Delta\omega$, where $\Delta\omega$ is the sampling frequency interval and k is a frequency index set, one derives that

$$\underline{y}_k(\underline{\theta}) = \sum_{r=1}^{m}[\underline{u}_r\underline{l}_r^T\underline{\eta}_k(\lambda_r) + \underline{u}_r^*\underline{l}_r^{*T}\underline{\eta}_k(\lambda_r^*)] + D_c\underline{\ddot{z}}_k + \sum_{r=1}^{m}[(\underline{\alpha}_r + \underline{b}_r e^{-jk\Delta\omega T})A_k(\lambda_r) + (\underline{\alpha}_r^* + \underline{b}_r^* e^{-jk\Delta\omega T})A_k(\lambda_r^*)] \tag{13}$$

where, $\underline{\alpha}_r = \underline{u}_r\xi_r(0) \in \mathrm{C}^{N_{out}\times 1}$, $\underline{b}_r = -\underline{u}_r\xi_r(T) \in \mathrm{C}^{N_{out}\times 1}$,

$$\underline{\eta}_k(\lambda_r) = \frac{\underline{\hat{\ddot{z}}}(k\Delta\omega)}{jk\Delta\omega - \lambda_r}, \qquad A_k(\lambda_r) = -\frac{1}{jk\Delta\omega - \lambda_r} \qquad \text{and} \qquad \underline{\ddot{z}}_k = \underline{\hat{\ddot{z}}}(k\Delta\omega) \tag{14}$$

From the structure of the response function in (13), the parameter set $\underline{\theta} = \{\lambda_r, \underline{u}_r, \underline{l}_r^T, \xi_r(0), \xi_r(T), r = 1, ..., m, D_c\}$ completely defines the acceleration response at the measured DOFs using m complex modes. Also, introducing the functions

$$g_k(\underline{\theta}_r^a) = \underline{l}_r^T\underline{\eta}_k(\lambda_r) + [\xi_r(0) - \xi_r(T)e^{-jk\Delta\omega T}]A_k(\lambda_r) \tag{15}$$

$$h_k(\underline{\theta}_r^a) = \underline{l}_r^{*T}\underline{\eta}_k(\lambda_r^*) + [\xi_r^*(0) - \xi_r^*(T)e^{-jk\Delta\omega T}]A_k(\lambda_r^*) \tag{16}$$

equation (13) can also be written in an alternative convenient form

$$\underline{y}_k = \sum_{r=1}^{m} [\underline{u}_r g_k(\underline{\theta}_r^a) + \underline{u}_r^* h_k(\underline{\theta}_r^a)] + D_c \ddot{\underline{z}}_k \tag{17}$$

where the parameter set $\underline{\theta}_r^a$ is defined by

$$\underline{\theta}_r^a = (\underline{l}_r, \lambda_r, \xi_r(0), \xi_r(T)) \tag{18}$$

The importance of the alternative form (17) will be made clear in the next section.

4. Least Squares Identification of Structural Modes in Frequency Domain

A modal model output least-squares error identification approach seeks the optimal values of the parameter set $\underline{\theta}$ that minimize a measure of fit between the modal model predictions $\underline{y}_k(\underline{\theta})$, $k = 1, \cdots, N$ and the corresponding response $\hat{\underline{y}}_k$ estimated from the measured data. That is, the modal model identification is formulated as a minimization problem of finding the values of $\underline{\theta}$ that minimizes the weighted measure of fit

$$J(\underline{\theta}) = \frac{1}{V} \sum_{k=0}^{N} \left[\underline{\varepsilon}_k^{NL} \right]^T W \left[\underline{\varepsilon}_k^{NL} \right] = \frac{1}{V} \sum_{k=0}^{N} \left\| \underline{\varepsilon}_k^{NL} \right\|^2 \tag{19}$$

where the error $\underline{\varepsilon}_k^{NL}(\underline{\theta})$ between the measured and modal model predicted responses

$$\underline{\varepsilon}_k^{NL}(\underline{\theta}) = \underline{y}_k(\underline{\theta}) - \hat{\underline{y}}_k \tag{20}$$

is a nonlinear function of the parameter set $\underline{\theta}$, N is the number of sample data over the analyzed time period T (response duration), and $V = \sum_{k=0}^{N} \left\| \hat{\underline{y}}_k \right\|^2$ is the normalization factor, and $\left\| \underline{y} \right\|^2 = \underline{y}^T W \underline{y}$ with $W \in R^{N_{out} \times N_{out}}$ being a user selected weighting matrix. Herein, it is selected to be the identity matrix, $W = I$.

From the computer implementation point of view, it is necessary to describe the response vector $\underline{y}_k(\underline{\theta})$ in terms of real-valued variables and parameter set $\underline{\theta}$. For this, the complex-valued scalar and vector variables $\underline{u}_r$, $\underline{l}_r$, $\xi_r(t)$ and $\xi_r(0)$ involved in the description of the modal model are expressed in terms of the real and imaginary parts. The total number of model parameter involved in the prediction of the response at N_{out} DOFs given m modes and N_{in} base input time histories, is $\left[4m + 2(m \times N_{in}) + 2(N_{out} \times m) + (N_{out} \times N_{in}) \right]$.

4.1 Optimization algorithm

A three step approach is used to estimate the modal properties by solving the least-squares optimization problem.

4.1.1 Step 1: Identification of modes and estimation of modal frequencies and damping ratios

The first step provides estimates of the modal frequencies and modal damping ratios by re-formulating the objective (error) function in a convenient way so that these modal properties can be obtained by solving a system of linear algebraic equations using the common denominator model [17]. Stabilization diagrams are used as part of the approach to distinguish between physical and mathematical modes and automatically estimate the number of contributing modes. This first step is an extension of the PolyMAX or polyreference least-squares complex frequency domain method [18]. It is employed herein to treat non-classically damped modal models describing the system's response characteristics based on earthquake-induced vibration data. Details are presented in Nikolaou [15]. Stabilization diagrams can be used to distinguish between the mathematical and the physical modes and eventually keep only the physical modes of the system. Thus the first step not only provides estimates of the modal frequencies and modal damping ratios but also gives the number of contributing modes through the appropriate-conventional use of stabilization diagrams.

4.1.2 Step 2: Estimation of mode shapes and participation factors

In the second step, the number of contributing modes m and the estimated values of the poles λ_r are considered to be known and are used with (13) or (17) in order to obtain estimates of the remaining unknown modal parameters, the mode shapes $\underline{u}_r$, the participation factors $\underline{l}_r$, the real matrix D_c, and the vectors $\underline{a}_r$ and $\underline{\beta}_r$ or the initial conditions $\xi_r(0)$ and $\xi_r(T)$. Two different approaches have been developed for the computation of these quantities in the second step.

In the first approach, estimates of the residue matrices $R_r = \underline{u}_r \underline{l}_r^T$, the real matrix D_c, and the vectors $\underline{a}_r$ and $\underline{\beta}_r$ are obtained by minimizing (19) with $\underline{\varepsilon}_k^{NL}(\underline{\theta})$ given by (20) and $\underline{y}_k(\underline{\theta})$ given by (13) with $\underline{u}_r \underline{l}_r^T$ replaced by R_r. It is evident from the structure of the problem that the objective function is quadratic in the elements R_r, D_c, $\underline{a}_r$ and $\underline{\beta}_r$. So one can develop a system of linear equations for the elements R_r, D_c, $\underline{a}_r$ and $\underline{\beta}_r$ [15]. Given the residue matrix R_r and noting that it admits the representation $R_r = \underline{u}_r \underline{l}_r^T$, i.e. is expected to be of rank one, the mode shapes $\underline{u}_r$ and the modal participation factors $\underline{l}_r$ are derived directly by the Singular Value Decomposition (SVD) for the resulting numerator matrices R_r using the left-hand and right-hand singular vectors corresponding to the highest singular value.

The second approach is based on the form (17) for the response predictions $\underline{y}_k(\underline{\theta})$. In this case the parameters to be identified are $\underline{u}_r$, $\underline{l}_r$, $\xi_r(0)$, $\xi_r(T)$, $r = 1, \cdots, m$, and the real matrix D_c. The total number of parameters is $2m(1 + N_{out} + N_{in}) + N_{out} N_{in}$ for non-classically damped modal models. The total number of parameters can be reduced to $2m(1 + N_{in})$, containing the parameters $\underline{l}_r$, $\xi_r(0)$ and $\xi_r(T)$ for each mode by recognizing that the objective function in (19) is quadratic with respect to the complex mode shape $\underline{u}_r$ and the real matrix D_c. Applying the optimality conditions in (19) with respect to the components of $\underline{u}_r$ and D_c, a linear system of equations results for obtaining $\underline{u}_r$ and D_c with respect to the parameters $\underline{l}_r$, $\xi_r(0)$ and $\xi_r(T)$. This system of equations is given in Nikolaou (2008). The resulting nonlinear optimization problem with respect to the remaining $2m(1 + N_{in})$ parameters $\underline{l}_r$, $\xi_r(0)$ and $\xi_r(T)$, $r = 1, \cdots, m$, is solved in Matlab using available gradient-based optimization algorithms.

4.1.1 Step 3: Modal estimation by full nonlinear optimization

The two-step approach gives results that are very close to the optimal estimates. However, for closely spaced and overlapping modes, the two step approach may not be adequate. In this case it is recommended to solve the full nonlinear optimization problem for the identification of all modal parameters simultaneously. Specifically, the modal parameters in the set $\underline{\theta}$ are identified by minimizing the objective function (19) with $\underline{\varepsilon}_k^{NL}(\underline{\theta})$ given by (20). The modal parameter set $\underline{\theta}$ to be identified contains the parameters ω_r, ζ_r, $\underline{u}_r$, $\underline{l}_r$, $\xi_r(0)$, $\xi_r(T)$, $r = 1, \cdots, m$, and the real matrix D_c that completely define the response vector in (17). The total number of parameters is $2m(2 + N_{out} + N_{in}) + N_{out} N_{in}$ for non-classically damped modal models.

The minimization of the objective function (19) can be carried out efficiently, significantly reducing the computational cost, by recognizing that the error function in (19) is quadratic with respect to the complex modeshapes $\underline{u}_r$ and the elements in the matrix D_c. This observation is used to develop explicit expressions that relate the parameters $\underline{u}_r$ and D_c to the vectors $\underline{l}_r$, the modal frequencies ω_r, the damping ratios ζ_r, and the

initial conditions $\xi_r(0)$, $\xi_r(T)$ so that the number of parameters involved in the optimization is reduced to $2m(N_{in}+2)$. This reduction is considerable for a relatively large number of measurement points. Applying the optimality conditions with respect to the components of $\underline{u}_r$ and D_c, a linear system of equations results for obtaining $\underline{u}_r$ and D_c with respect to the ω_r, ζ_r, $\underline{l}_r$, $\xi_r(0)$ and $\xi_r(T)$, $r=1,\cdots,m$. This linear system is given in Nikolaou [15]. The resulting nonlinear optimization problem with respect to the remaining variables $\underline{l}_r$, ω_r, ζ_r, $\xi_r(0)$ and $\xi_r(T)$, $r=1,\cdots,m$, is solved in Matlab using available gradient-based optimisation algorithms. The starting values of the parameters required in the optimization are obtained from the estimates provided by the first and second steps of the algorithm. These starting values are usually very close to the optimal values for most of the modes and thus the optimization algorithm converges in a relatively few iterations. The derivatives of the objective function with respect to the modal parameters are evaluated analytically, accelerating the convergence of the algorithm.

5. Application to Alcazar Building

5.1 Building description, instrumentation and vibration measurements

The Alcazar building shown in Fig. 1 is a sixteen-story building office located in the city of Viña del Mar, Chile. The building is 30 m by 35 m in plan and it has three underground floors (parking facilities). It is approximately 50 m tall. The first story is 3.42m in height and stories 2-16 are 3.24m in height. The Building was built in 2008 according to the 2004 Chilean Building Code (NCh 433). The lateral force resisting system consists of a perimeter reinforced concrete moment frame in both directions and shear walls in the NS direction. In addition the building has a reinforced concrete core shear walls in the middle. In summary the gravity system comprises a reinforced concrete slab supported by the core shear walls, eight rectangular columns of a perimeter frame, and four shear walls located at the perimeter. A high fidelity FE model is developed in SAP. The floors and the walls are modeled with shell elements of different thicknesses. For instance the shear walls of the concrete core are modeled with elements of thickness equal to 0.4m while the shell elements that model the shear walls at the perimeter have a thickness equal to 0.5m. Additionally, beam and column elements are used in the FE model which has approximately 60000 DOF. The FE model is depicted in Fig. 2.

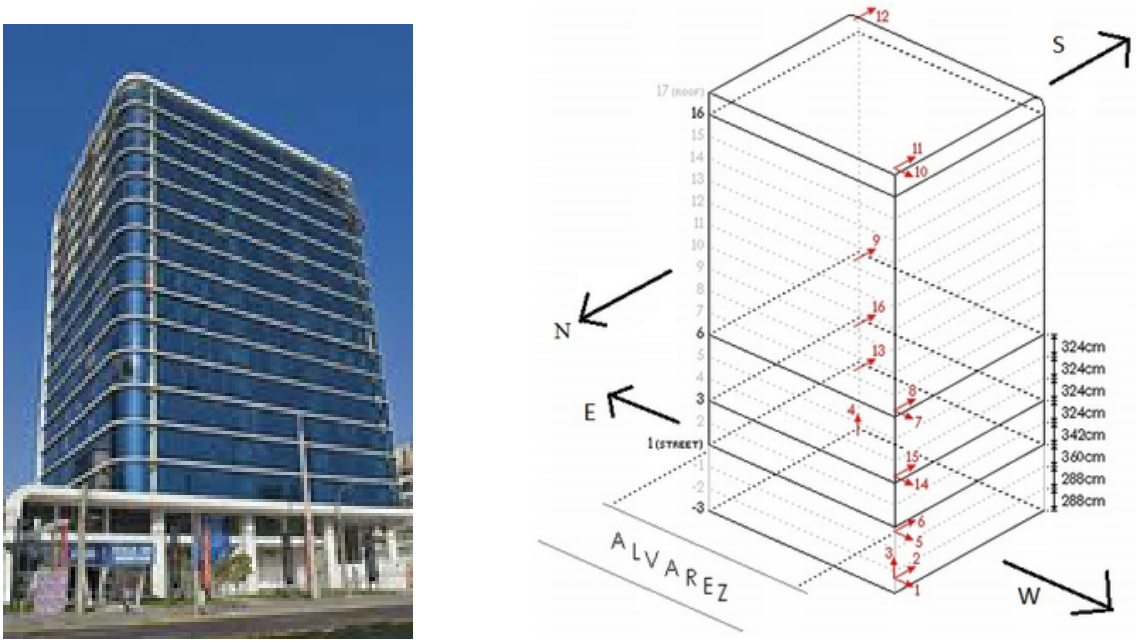

Fig. 1 – Alcazar building (left) and instrumentation (right)

The 16-story building was instrumented with an array of 12 acceleration sensors. The instrumentation is shown in Fig. 1 (right). Four (4) sensors were installed in the underground level (level -3), three (3) in the ground level (level 0), and from three (3) in the third, sixth and top floor. The two vertical sensors 3 and 4 in the underground floor were not activated. The sensors are measuring along the two horizontal directions of the building, one sensor in the EW direction and two in the NS direction so that torsional modes are identified. There are no sensors available in the intermediate floors (from 7th to 16th), making it very challenging to identify the type of modes and correlate the modes with a FE model. The sampling rate for the corrected accelerograms is 0.01 sec.

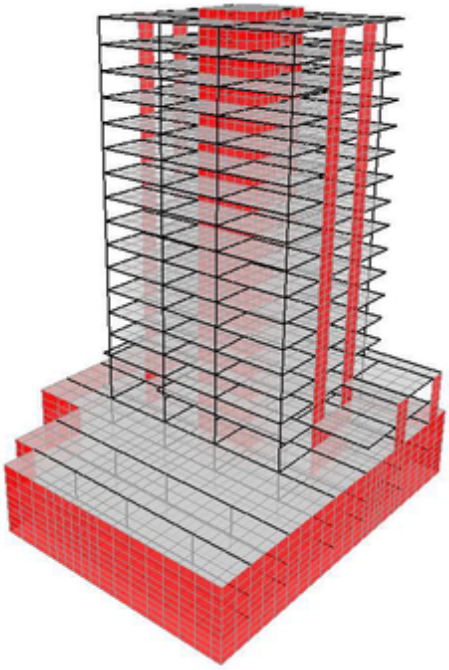

Fig. 2 – FE model of the Alcazar building

5.2 Modal identification

Recordings are available from three earthquake events that occurred at April 5, 2010 (Event 1), May 1, 2010 (Event 2) and March 17, 2011 (Event 3). To get a feel of the vibration levels of each event, the time history of the horizontal earthquake accelerations at the underground level (level -3) and the top floor (level 17) in both directions is given in Fig. 3 and 4, respectively. It can be observed that Event 2 is slightly stronger than Event 3, while the vibration levels of Event 1 are approximately 30% to 40% lower than the vibration levels of Event 3.

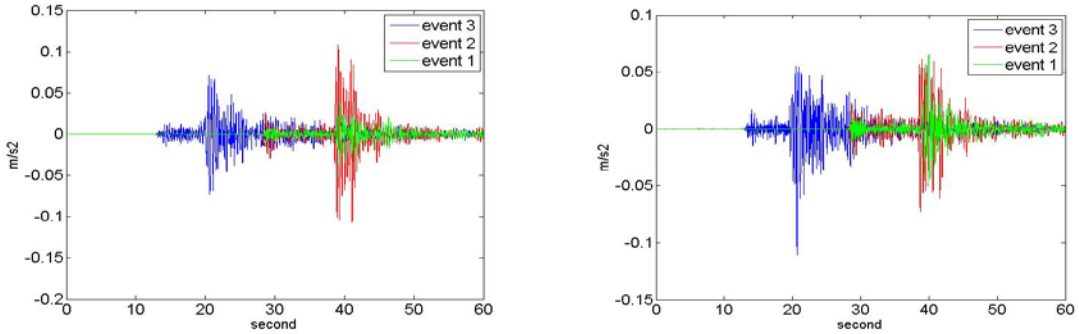

Fig. 3 – Acceleration for the three events at the underground level for sensor 1-EV (left) and sensor 2-NS (right)

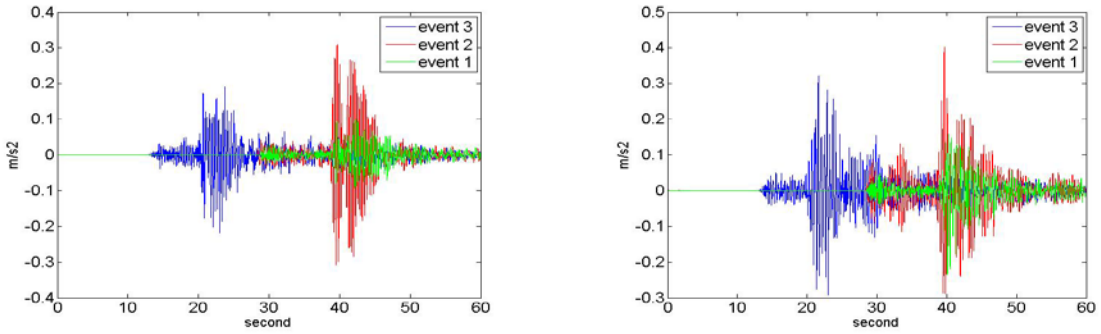

Fig. 4 – Accelerations for the three events at the top floor for sensor 11-EW (left) and sensor 12-NS (right)

Modal identification results are next presented. Using stabilization diagrams (Step 1) as well as visual inspection of the Fourier transforms of the output accelerations only a small number of modes is identified from these low amplitude earthquake recordings. The values of the modal frequencies and the modal damping ratios of the identified modes for each low-amplitude earthquake event are shown in Table 1. It is noted that from five (5) to six (6) modes were successfully identified from combined analysis of the three low amplitude earthquake events: three bending modes in the NS-direction (NS), two bending modes in the EW-direction and the second torsional mode. The modes were identified to be very close to classically-damped modes. Due to the sparse sensor grid and the absence of sensors from the 7th up to the 16th floor of the building, the type of some of the modes could not be estimated with certainty without the use of the FE model as a guide. The modal frequencies computed by the FE model of the building are also shown in the last column of Table 1.

Table 1 – Modal frequencies and damping ratios of the identified and FE predicted modes

	Event 1		**Event 2**		**Event 3**		**FE model**
Type of Mode	**ω (Hz)**	**ζ (%)**	**ω (Hz)**	**ζ (%)**	**ω (Hz)**	**ζ (%)**	**ω (Hz)**
1st Bending (NS-dir)	-	-	0.677	2.92	-	-	0.74
1st Bending (EW-dir)	0.832	0.93	0.831	1.46	0.826	1.96	0.81
1st Torsional	-	-	-	-	-	-	1.00
2nd Bending (NS-dir)	2.45	2.51	2.75	0.48	2.46	2.47	2.75
2nd Torsional	3.29	1.06	3.24	1.34	3.24	2.66	3.34
2nd Bending (EW-dir)	4.00	1.71	-	-	-	-	3.70
3rd Bending (NS-dir)	5.11	1.98	5.01	2.32	5.10	2.43	5.56

The analysis of the three seismic events gave results for the modal frequencies and damping ratios that are consistent. It is observed that most of the identified modal frequencies have relatively small variation over the three low-amplitude seismic events. Despite the fact that event 2 is 30 to 40% weaker than Events 1 and 3, there is no noticeable difference in the modal frequencies which one can conclude that the building performed in the linear range under all three events and there is no activation of nonlinear mechanism from these three events. The identified modal frequencies are also consistent with the modal frequencies predicted by the high fidelity FE model, although the FE model appears stiffer due to the higher values of the predicted modal frequencies than the ones identified from the actual building behavior. The modal damping ratios range from 1 to 2% for the 1st bending mode in the EW direction, from 0.5 to 3% for the lowest three bending modes in the NS directions and

the torsional mode. This could be considered consistent with literature results for this low-amplitude vibration levels experienced by the building.

The identified modes are representative of the condition of the building at low-amplitude vibration levels and can be used for calibrating the FE model of the building. Also, combined with future measurements from stronger earthquake events, they can be used for linear and nonlinear FE analyses as well structural health monitoring purposes. It should be noted that model updating should be mainly based on identified modal frequencies. Matching the mode shapes presents difficulties mostly due to the fact that there are no measurements available from the 7th up to the 16th floor of the building. FE model updating using hierarchical Bayesian modeling, which can be used to account for the variability of the modal frequencies identified from the three seismic events, is left for a future work.

Fig. 5 compares the FT of the measured accelerations and the FT of the accelerations predicted by the identified optimal modal model for representative frequency ranges. In most cases, the fit of the measured power spectral density is very good which validates the effectiveness of the proposed modal identification method.

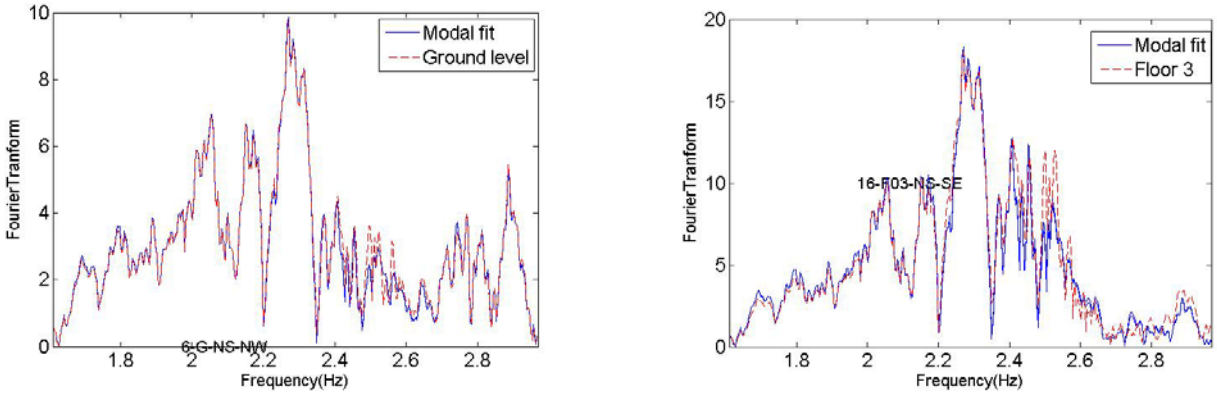

Fig. 5 - Comparison of FT of accelerations between measured and identified optimal modal model for sensors 6 and 16 (Event 3)

6. Conclusions

Frequency domain least squares methods for the identification of non-classically-damped modal models of linear structures from multiple-support excitations and multiple responses were presented. The methods are extension of existing algorithms developed for classically-damped modal models. The identification involves the estimation of the number of contributing modes, the modal frequencies, the modal damping ratios, the complex mode shapes, the effective modal participation factors, the pseudo-response matrix, and the initial conditions of the contributing modes. Computational efficient algorithms for solving the resulting highly non-convex nonlinear optimization problems were proposed, including features of automatically estimating the number of contributing modes, as well as the modal frequencies and the damping ratios of the physical modes without or minimal user intervention. Specifically, a three-step approach was proposed to carry out efficiently the optimization in to improve accuracy of the modal characteristics for closely-spaced and overlapping modes. The proposed non-classically damped modal identification algorithms are applicable to the cases where the damping is not proportionally distributed throughout a structure. Such cases arise in base isolated building and bridges using local dissipation mechanics such as elastomeric bearings and viscous dampers. The modal identification method was applied to estimate the modal properties of the 16-story Alcazar building using base and output acceleration measurements from three different low magnitude earthquake event. A number of low-frequency modes were identified and compared with the modes predicted by a high-fidelity FE model. The identified modes are representative of the condition of the building at low vibration levels and can be used to calibrate FE models for the building to represent the dynamic characteristics at its current state. Currently, the effectiveness

of a hierarchical Bayesian modeling framework is explored for calibrating the stiffness properties and the uncertainties in the values of these properties of the FE model by taking into account the variabilities observed in the modal properties identified from the three seismic events.

7. Acknowledgements

This research has been implemented under the "ARISTEIA" Action of the "Operational Program Education and Lifelong Learning" and was co-funded by the European Social Fund (ESF) and Greek National Resources.

8. References

[1] Werner S.D., Beck J.L., Levine M.B. (1987): Seismic response evaluations of Meloland road overpass using 1979 Imperial Valley earthquake records. *Earthquake Engineering and Structural Dynamics*, **15**, 249-274.

[2] Vamvatsikos D, Cornell CA (2002): Incremental dynamic analysis. *Earthquake Engineering & Structural Dynamics*, **31** (3), 491-514.

[3] Safak E. (1995): Detection and identification of soil-structure interaction in buildings from vibration recordings. *Journal of Structural Engineering (ASCE)*, **121** (5), 899-906.

[4] Lus H., Betti R., Longman R.W. (1999): Identification of linear structural systems using earthquake-induced vibration data. *Earthquake Engineering and Structural Dynamics*, **28**, 1449–1467.

[5] Liu H., Yanga Z., Gaulkeb M.S. (2005): Structural identification and finite element modeling of a 14-story office building using recorded data. *Engineering Structures*, **27**, 463–473.

[6] Chaudhary M.T.A., Abe M., Fujino Y. (2000): System identification of two base-isolated buildings using seismic records. *Journal of Structural Engineering (ASCE)*, **126** (10), 1187-1195.

[7] Chaudhary M.T.A., Abe M., Fujino Y. (2002): Investigation of atypical seismic response of a base-isolated bridge. *Engineering Structures*, **24**, 945–953.

[8] Arici Y., Mosalam K.M. (2003): System identification of instrumented bridge systems. *Earthquake Engineering and Structural Dynamics*, **32**, 999–1020.

[9] Lin C.C., Hong L.L., Ueng J.M., Wu K.C., Wang C.E. (2005): Parametric identification of asymmetric buildings from earthquake response records. *Smart Materials and Structures*, **14**, 850-861.

[10] Beck J.L., Jennings P.C. (1980): Structural identification using linear models and earthquake records. *Earthquake Engineering and Structural Dynamics*, **8**, 145-160.

[11] McVerry G.H. (1980): Structural identification in the frequency domain from earthquake records. *Earthquake Engineering and Structural Dynamics*, **8**, 161-180.

[12] Papageorgiou A.S., Lin B.C. (1989): Influence of lateral-load-resisting system on the earthquake response of structures – A system identification study. *Earthquake Engineering and Structural Dynamics*, **18**, 799-814.

[13] Tan R.Y., Cheng W.M. (1993): System identification of a non-classically damped linear system. *Computers and Structures*, **46**, 67–75.

[14] Mahmoudabadi M., Ghafory-Ashtiany M., Hosseini M. (2007): Identification of modal parameters of non-classically damped linear structures under multi-component earthquake loading. *Earthquake Engineering and Structural Dynamics*, **36**, 765-782.

[15] Nikolaou I., (2008): Structural modal identification methods based on earthquake-induced vibrations. *MS Thesis Report No. SDL-08-2*, Department of Mechanical and Industrial Engineering, University of Thessaly, Volos, Greece.

[16] Clough R.W., Penzien J. (1993): *Dynamics of Structures*. McGraw-Hill.

[17] Heylen, W., Lammens, S., Sas, P. (1997): *Modal Analysis Theory and Testing*. Katholieke Universiteit Leuven, Department of Mechanical Engineering.

[18] Peeters B., Van der Auweraer H., Guillaume P., Leuridan J. (2004): The PolyMAX frequency-domain method: A new standard for modal parameter estimation?. *Shock and Vibration*, **11** (2-4), 395-409.